Comparison of the descriptions of yrast bands in the Harris and IBM models for even Th and U nuclei

A. D. Efimov[1,2†] I. V. Koval[1] I. N. Izosimov[3]

[1]Admiral Makarov State University of Maritime and Inland Shipping, St. Petersburg 198035, Russia,
[2]Ioffe Institute, St. Petersburg 194021, Russia
[3]Joint Institute for Nuclear Research, Dubna 141980, Russia,

Abstract: For even Th and U nuclei, the description of the energies of yrast bands in the Harris variable moment of inertia model is studied in its phenomenological application. For some of these nuclei, the results obtained in the microscopic version of the interacting boson model (IBM) are presented, in which high-spin excitation modes are also considered. For other nuclei, in scenarios where high-spin orbits are not highly significant in describing the properties of yrast bands, in addition to the Harris model, the IBM with a full standard Hamiltonian constructed only from *s* and *d* bosons is utilized. Because the Harris model is considered with no more than four parameters, it can be used for both heavy and superheavy nuclei to approximate the energies of high-spin states. This study on the properties of nuclei using various models reveals the possibilities of describing different behaviors of the moments of inertia in the IBM and outlines additional criteria for the implementation of band crossing.

Keywords: yrast bands, moments of inertia, Harris model, interacting boson model, Th, U

DOI: 10.1088/1674-1137/add25a **CSTR:** 32044.14.ChinesePhysicsC.49074108

I. INTRODUCTION

The visualization of the behavior of the energies of states E in a band becomes more qualitative if we move from energies to effective moments of inertia J. This also enables us to improve the method of comparing experimental and calculated energies of states of one band.

In addition, the backbending effect can be used to form judgments about the spin values at which the bands cross. A comparison of the $J(\omega^2)$ curves obtained from experimental energies with those given by various nuclear models, including microscopic ones, can reveal the capabilities of the corresponding models and provide more reasoned judgments about the nature and character of the states.

One of the methods of reproducing and predicting energies is based on the expansion of the moment of inertia in powers of the rotation frequency ω, as in the Harris model [1]. This is justified when the transition to a new band has not yet occurred in the rotation band. As a rule, such a transition occurs quite quickly in one or two states of the yrast band. In this case, this is shown on the graph of the moment of inertia versus the square of the rotation frequency in a specific manner through backbending. Among heavy nuclei, starting with thorium isotopes, three such nuclei are known today: ^{220}Th, ^{242}Pu, and ^{244}Pu. Hence, in Ref. [2], within the framework of the interacting boson model (IBM1) [3] phenomenology (hereinafter referred to as IBM), a good description of the energies of yrast bands up to extremely high spins I in heavy nuclei from Pu to No is presented. The effective moment of inertia and the square of the rotational frequency are defined as

$$\frac{2J}{\hbar^2} = \frac{4I-2}{E(I\to I-2)},$$
$$(\hbar\omega)^2 = \frac{\left(E(I\to I-2)\right)^2}{\left(\left(I(I+1)\right)^{1/2}-\left((I-2)(I-1)\right)^{1/2}\right)^2}. \quad (1)$$

This paper presents a description of the energies of yrast bands in even-even heavy nuclei in the Harris model, considered not from the perspective of the cracking model but as a phenomenological model with a number of parameters no more than four. The possibility of the IBM in its phenomenological aspect to describe moments of inertia is also considered. IBM phenomenology is understood as a description of the energies of collective states in nuclei through fitting the parameters both of the boson Hamiltonian and maximum number of quadrupole bosons. The moments of inertia obtained in the two models are compared. Finally, we aim to develop a cri-

Received 24 March 2025; Accepted 30 April 2025; Published online 1 May 2025

† E-mail: efimov98@mail.ru

terion for determining the spin at which the crossing of bands occurs. This can be performed based on a comparison of the behavior of $J(\omega^2)$according to experimental data and the results of the Harris model. Note that, in some cases, although backbending may not be observed, the crossing of bands is still possible. This was revealed by the microscopic description of the chain of isotopes $^{220\text{-}236}$Th [4]. The microscopic version of the IBM developed by us is presented in Ref. [4] and in the references therein. In this version, the boson parameters are calculated based on the effective factorized forces. In addition, owing to the expansion of the boson space by bosons with multipolarity up to to $J = 14^+$, it becomes possible to describe the phenomenon of band crossing in nuclei. Calculations within the Harris scheme are performed for all the presented nuclei. For ^{220,222}Th, the results are presented also within the IBM microscopic framework. For ^{226}Th and U isotopes, the IBM phenomenology is also used in calculations.

To increase the calculated moment of inertia at high-spin states in deformed nuclei (^{162,164}Er), Ref. [5] incorporated a new term into the Hamiltonian of the IBM such that $I(I+1) \to I(I+1)/(1+fI(I+1))$. This part of the Hamiltonian is always diagonal for any values of the parameters $H_{\rm IBM}$. This addition is motivated by the fact that a decrease in superfluidity, the gap parameter, leads to an increase in the moment of inertia, and the gap parameter decreases with increasing rotation frequency. This should lead to $\mathrm{d}J/\mathrm{d}I > 0$ and $\mathrm{d}J/\mathrm{d}\omega > 0$. However, note that the growth of the moment of inertia from the rotation frequency is achieved with arbitrary values of the traditional and full Hamiltonian of the IBM, except for the one that corresponds to the $SU(3)$ limit of the IBM. In addition, with the growth of the spin of the collective state, the influence of two-quasiparticle states on the energy of this state increases. An example of a band built on a two-quasiparticle mode is the S band. This also leads to an additional increase in the moment of inertia or a decrease in the energies of intra-band transitions.

An analysis of the dynamic moments of inertia of the lowest superdeformed (SD) bands in even-even Hg, Pb, Gd, and Dy [6] as well as ^{192,194}Hg and ^{152,154}Dy [7] isotopes revealed the need to extend the coefficient f such that, considering only the relative excitation of the states in a rotational band, the energy of the state with angular momentum I can be simply expressed as

$$E(I) = \frac{C_0}{1 + f_1 I(I+1) + f_2 I^2 (I+1)^2} I(I+1).$$

The introduction of an additional modification of the Arima coefficient f shows that J can change nonmonotonously with rotational frequency up to a point such that, as the spin increases, the positive slope of the moment of inertia from the rotation frequency can become negative. This phenomenon, analogy with the terms "backbending" and "upbending" can be called downbending.

Calculations on this basis belong to semi-phenomenological approaches.

In Ref. [8], a novel modification was introduced to extend the Arima coefficient to the third order. The computed outcomes of the rotational bands of ^{244}Pu and ^{248}Cm demonstrated an exceptional degree of agreement with experimental observations. Moreover, the used parameterization of the Arima term and its modification successfully describes such behavior of the moment of inertia from frequency as backbending, upbending, and the downturn (down bending).

As noted in earlier reports [5–8], the phenomenon of backbending is traditionally associated with the intersection of bands of different nature, namely, the collective one, built on the ground state, and the one that has a two-quasiparticle pair with a sufficiently high spin at its base.

The upbending phenomenon may be due to the crossing of bands not having occurred completely, although the system appears to be close to that point. In addition, the growth of the slope of the moment of inertia from frequency within certain limits is reproduced within the framework of the traditional but complete IBM Hamiltonian.

From a microscopic perspective, as the spin of states increases, the average number of quadrupole bosons increases, and this leads to some weakening of pairing. Accordingly, the introduction of the Arima modification of the IBM Hamiltonian was motivated by this decrease in pairing correlation owing to the increase in rotation. Additionally, this leads to an increase in the energy of the quasiparticle vacuum or a decrease in the correspon ding depth.

Here, with an increase in the spin of the collective state, the microscopically calculated energy of the d boson ε_d decreases (the corresponding term also occurs when using only the $\hat{Q}\cdot\hat{Q}$ interaction by reducing the last operator to the normal order over bosons). Because the IBM assumes that the energy of the boson vacuum is constant, the variable part of the energy of the quasiparticle vacuum is redistributed over two boson parameters ε_d and k_1 [see below (8)]. This results in the d-boson energy practically ceasing to change and the energy of the boson vacuum remaining unchanged. This procedure is described in Refs. [9–11] and clearly demonstrated in Ref. [11].

Thus, the weakening of pairing during the unwinding of the nucleus by the values of the parameters of the boson Hamiltonian is significantly leveled out.

One more effect occurs: this is the weakening of the growth of the moment of inertia with frequency at high spins − downturn or downbending. We can assume that the IBM specificity, namely, the finiteness of the maximum number of quadrupole bosons, can reproduce this

phenomenon [12] without introducing the Arima modifications to the boson Hamiltonian. Introducing the Arima modification is convenient if we remain in the $SU(3)$ approximation of the IBM limit. Thus, this modification approximates a more complex dynamics of collective motions in the nucleus, described in the general case by the $SU(6)$ group.

In Ref. [13], the structure of yrast bands in the transuranium nuclei ^{242}Pu and ^{244}Pu was investigated within the framework of the projected shell model. This approach is completely microscopic.

The description of rotational bands at ultra-high spins within the framework of covariant density functional theory for the $A \geq 242$ actinides is presented in Ref. [14].

The rotational band properties of plutonium isotopes $^{236\text{-}246}$Pu were studied [15] via the projected shell model. The results of the calculated energy levels of the yrast band were compared with experimental data, and a good agreement was found. The crossing between two-quasiparticle (2qp) excited bands and the ground state band (g-band) in the high-spin regions was analyzed in terms of band diagrams. The upbendings were observed in the kinematic moments of inertia curves for $^{236\text{-}246}$Pu isotopes.

The objectives of this work are defined as follows:

1) obtaining a precise description of the energies of yrast bands in even-even heavy nuclei in the Harris model;

2) comparison of the behavior of $J(\omega^2)$ in the Harris and IBM models both in its phenomenological aspect and in the aspect of its extension by considering high-spin modes;

3) development of a criterion for determining the spin at which the crossing of bands occurs without resorting to microscopic calculations;

4) identification of the causes, conditions, and values of the spins of collective states when the downturn or downbending effect occurs.

II. PHENOMENOLOGICAL VARIANT OF THE HARRIS MODEL

We will use the Harris model [1] in its phenomenological aspect. If we assume that the following decomposition is valid

$$\sqrt{I(I+1)} = \omega\left(J_0 + \frac{2}{3}J_1\omega^2 + \frac{3}{5}J_2\omega^4 + \frac{4}{7}J_3\omega^6 + \ldots\right), \quad (2)$$

then the effective moment of inertia will have the form

$$J = J_0 + J_1\omega^2 + J_2\omega^4 + J_3\omega^6 + \ldots \quad (3)$$

With fixed values of parameters J_0, J_1, J_2, J_3, the rotation frequencies are determined from the equation

$$\frac{2J_0}{\hbar^2} + \frac{2J_1}{\hbar^4}(\hbar\omega)^2 + \frac{2J_2}{\hbar^6}(\hbar\omega)^4 + \frac{2J_3}{\hbar^8}(\hbar\omega)^6 = \frac{2(2I-1)}{\left(\sqrt{I(I+1)} - \sqrt{(I-2)(I-1)}\right)\hbar\omega}. \quad (4)$$

For each value of the spin of state I, the value $\omega = \omega_I$ is determined. The energies of the states of the main band are determined as

$$E_I = E_{I-2} + \left(\sqrt{I(I+1)} - \sqrt{(I-2)(I-1)}\right)\hbar\omega, \quad (5)$$

where $E_0 = 0$. The parameters that determine the moment of inertia (3) are found by minimizing the value

$$\chi^2 = \sum_I (E_I^{(\exp)} - E_I)^2 \quad (6)$$

or the standard deviation

$$\sigma = \sqrt{\frac{\sum_I^{I_{\text{fit}}} (E_I^{(\exp)} - E_I)^2}{I_{\text{fit}}/2}}, \quad (7)$$

where I_{fit} is the maximum spin of the states, and the bands by which the parameters J_0, J_1, J_2, J_3 are determined.

The results obtained using the Harris model are related to the results in the IBM phenomenology. The parameterization of its Hamiltonian is expressed as

$$H_{\text{IBM}} = \varepsilon_d\, \hat{n}_d + k_1(d^+ \cdot d^+ ss + \text{H.c.}) + k_2\left((d^+d^+)^{(2)} \cdot ds + \text{H.c.}\right) + \frac{1}{2}\sum_L C_L(d^+d^+)^{(L)} \cdot (dd)^{(L)}, \quad (8)$$

H.c. means Hermitian conjugation, the dot between the operators corresponds to the scalar product, and the quantities $\varepsilon_d, k_1, k_2, C_0, C_2, C_4$ are the parameters of the model. The total number of bosons or maximum number of d bosons is denoted as Ω. For several nuclei, results are presented within the framework of the extended microscopic version of the IBM, where high-spin excitation modes are also considered; the corresponding content is not disclosed here, but further deails can be found in Ref. [4].

The next section discusses the energies of the yrast band states of even thorium isotopes in comparison with the results of the Harris model phenomenology, and for several nuclei with the IBM.

III. ANALYSIS OF MOMENTS OF INERTIA FOR EVEN ISOTOPES OF Th

Figure 1 presents a visual systematics of the energies

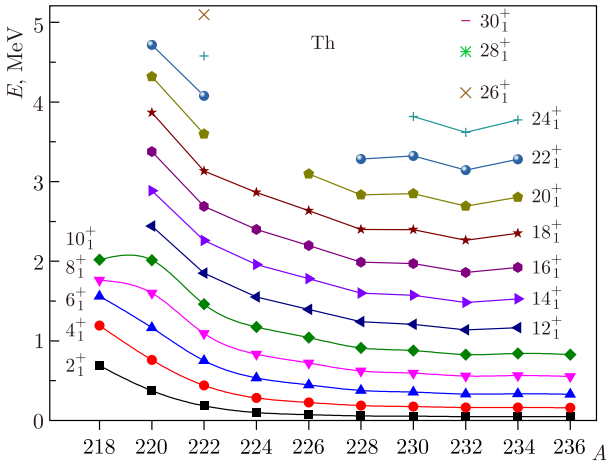

Fig. 1. (color online) Energies of states of the yrast band in even isotopes of thorium.

of the corresponding states. The energies of states with spins $I \le 10^+$ initially decrease to $A = 224$ rather quickly, and at large nucleon values, the energies decrease quite smoothly, such that $E(2_1^+) = 48.4$ keV for ^{236}Th. The minimum energy of states with spins $I \ge 12^+$ is achieved in the ^{232}Th nucleus.

In Fig. 2, for all even thorium isotopes considered, the effective moments of inertia obtained from the experimental and calculated energies in the variable moment of inertia model, denoted as Harr, are compared. For two nuclei, ^{220,222}Th, the results of calculations in the IBM microscopic version, extended by high-spin excitation modes up to spins 14^+, are also given and denoted as IBM-qp. The parameters determining the values of the moments of inertia are given in Table 1, where the standard deviations of the calculated values of energies from the experimental ones are also given relative to the states for which the parameters were selected, the spins of the states to which the parameters are selected, and the maximum spin in the band. For the ^{226}Th nucleus, the results of calculations within the framework of the IBM phenomenology are also presented.

For the lightest of the thorium isotopes under consideration, ^{220}Th, backbending is observed starting from spin 10^+, and because the Harris model does not claim to describe it, the parameters are determined from transitions until the state with 8^+. The energies in ^{220}Th in the lower part of the spectrum up to spin 8^+ are perfectly reproduced by the $SU(5)$ limit of the IBM. Therefore, these states have no relation to the rotation of the deformed core. This corresponds to the negative value of the parameter J_0 in Table 1. Nevertheless, the representation of the energies of collective bands through moments of inertia is also very convenient in these cases. In the follow-

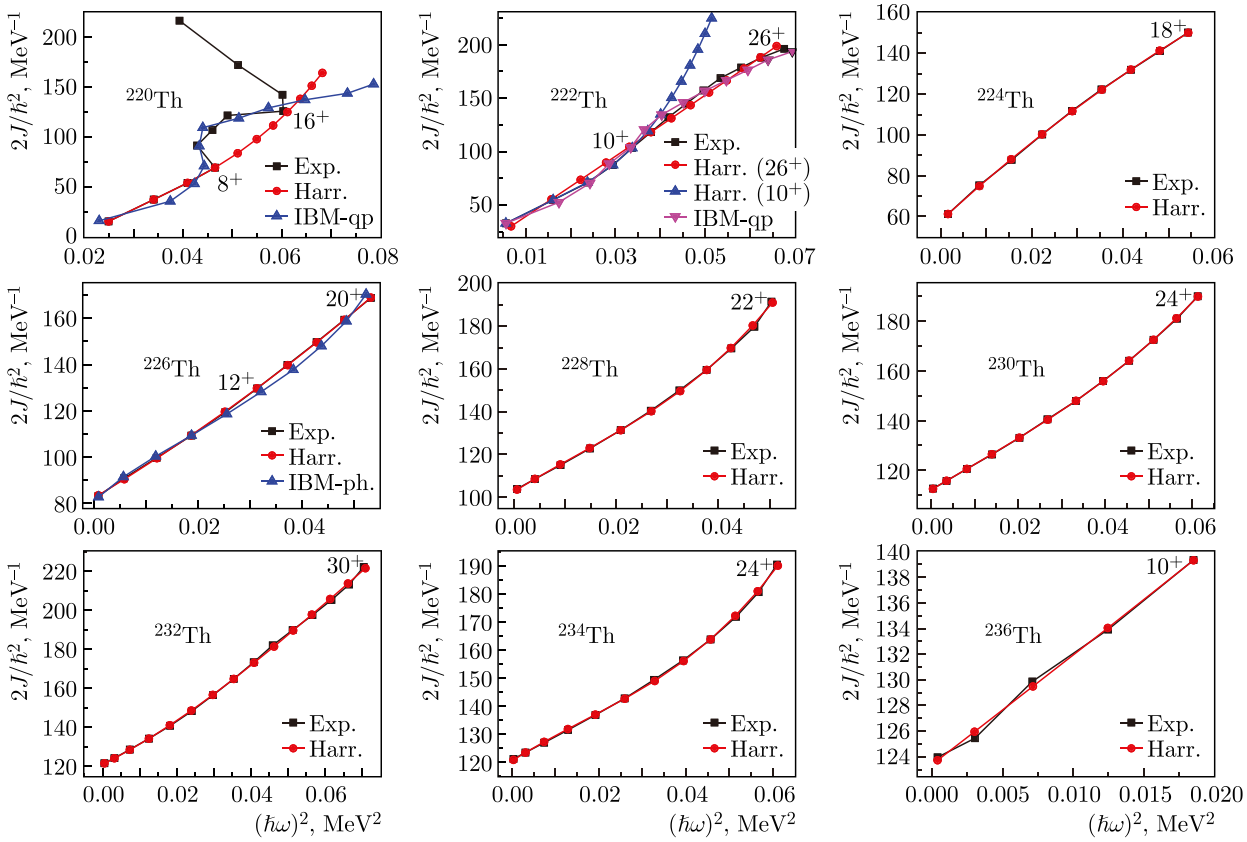

Fig. 2. (color online) Effective moments of inertia from experimental and theoretical energy values of yrast bands in Th isotopes.

Table 1. Parameters determining the effective moments of inertia for Th and U isotopes.

Nucleus	$2J_0/\hbar^2$	$2J_1/\hbar^4$,	$2J_2/\hbar^6$	$2J_3/\hbar^8$	σ	$I_{\rm fit}$	$I_{\rm max}$
	MeV^{-1}	MeV^{-3}	MeV^{-5}	MeV^{-7}	keV		
^{220}Th	-78.027	5627.16	-100806	1032727	0.14E-02	8	22
^{222}Th	11.116	2788.26	865.45	0	9.59	26	26
	17.465	3172.00	-85959.8	1995659.8	0.172	10	26
^{224}Th	57.965	2058.09	-7175.0	9656.4	0.33	18	18
^{226}Th	82.233	1369.23	4017.6	15137.6	0.33	20	20
^{228}Th	102.731	1474.68	-12333.3	349536.8	0.59	22	22
^{230}Th	112.141	1038.92	-2054.2	94199.8	0.175	24	24
^{232}Th	121.107	928.66	10424.0	-50092.3	0.89	30	30
^{234}Th	120.341	984.69	-10471.4	212984.7	0.63	24	24
^{236}Th	123.400	844.93	772.3	0	0.18	10	10
^{226}U	71.87581	1598.41785	6953.44873	-118350.98438	0.294	14	14
^{230}U	115.33965	1119.44153	-3171.23999	121410.60156	0.262	22	22
^{232}U	125.72275	944.34747	3252.86279	64539.00781	0.124	20	20
^{234}U	137.59946	1030.29688	14549.98926	-126356.42969	0.35	30	30
^{236}U	133.45268	385.92599	19432.23242	-89088.77344	1.90	30	30
^{236}U	132.30104	781.21796	-1048.02319	172107.54688	0.155	24	30
^{238}U	133.00563	941.80017	-9015.27832	267665.18750	0.468	28	34
^{240}U	132.39108	388.02209	14673.71387	0.00000	0.413	12	12

ing isotopes, this parameter is positive, and as the collectivity increases, *i.e.*, as the energy of the states decreases, J_0 increases. Here, in the theory that explicitly considers the elementary modes of two-quasiparticle excitations with high spins [4, 16], the behavior of the moment of inertia associated with the first backward bend is reproduced. This is demonstrated in Fig. 2. Figure 3 shows the composition of wave functions, whose components include collective states constructed only from d bosons corresponding to the lowest quadrupole excitations, as well as components including bosons b_J with high multipolarities. In Fig. 3, for ^{222}Th, the only component with b_8 that makes noticeable contributions to the wave functions of states, in addition to the collective one determined only by d bosons, is the component with b_8. No direct channel exists for the interaction of collective states with those containing the b_8 boson. The interaction is achieved through the components with b_J, $J = 2,4,6$. The latter components contribute to the renormalization of the traditional IBM Hamiltonian. Only two components are distinguished for thorium isotopes in the boson representation. If the wave function were represented in terms of D and B phonons, the component with only D phonons would be smaller, and the components with B_4 and B_6 phonons would be significant. Note that, in the presented calculations, the strong indirect interaction of the two components weakly depends on a reasonable

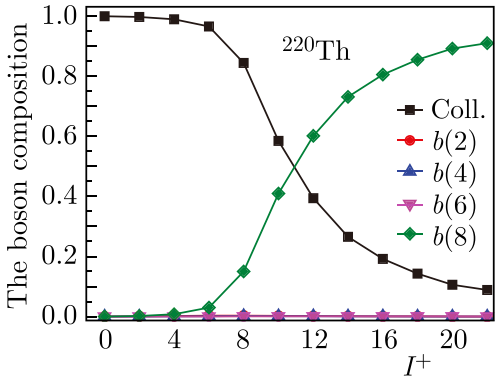

Fig. 3. (color online) Composition of the wave functions of the states of the yrast band obtained based on the microscopic model of ^{220}Th.

change in the position of the B_8 phonon energy. According to this figure, for the 8^+ state, the collective component composed only of d bosons is greater than 50%. The second backbending, corresponding to the 18^+ spin, should be attributed to the four-quasiparticle excitation.

For the ^{222}Th isotope, no manifestation of the bands crossing is observed. However, the average discrepancy between the calculated energies within the Harris and experimental schemes is significantly larger than that for heavier thorium isotopes, as follows from Table 1. The reason for this is that although no backbending is ob-

served in this nucleus, a smooth crossing of bands still occurs, as shown in Ref. [4]. This is demonstrated in Fig. 2, corresponding to ^{222}Th, where the moments of inertia obtained based on the microscopic calculation are also given. Figure 4 shows the composition of the wave functions. According to this figure, for the 12^+ state, ψ^2(coll) is approximately equal to 50%. Therefore, according to the Harris method, in addition to calculations for all energy differences up to the state with spin 26^+, calculations were made considering the states up to the state with spin 10^+. In the first case, the difference between the calculated and experimental values up to spin 8^+ is less than 1 keV, and for 10^+, it is already 5.5 keV. In the second case, this difference for 2^+, $4^+$is approximately 2 keV, but for the remainder, up to 14^+, it is less than 1 keV. Together with the previous thorium isotope, this shows that the Harris energy calculation procedure can be successfully applied if the collective component in the wave function is greater than 50%.

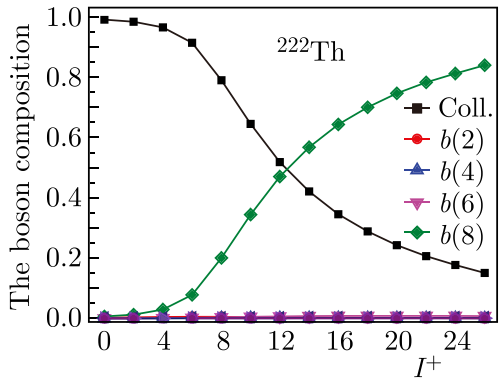

Fig. 4. (color online) Composition of the wave functions of the states of the yrast band obtained on the basis of the microscopic model for ^{222}Th.

For all nuclei, starting with ^{224}Th, in the Harris scheme, an accuracy of reproduction of experimental energies has been achieved such that the difference between the calculated and experimental energies does not exceed 1 keV on average, as can be observed from the σ values given in Table 1. This corresponds to Ref. [4], which showed that, in thorium isotopes, starting with this one, in all observed states of yrast bands, the collective component remains the main component. The calculated energies obtained in the Harris scheme in Tables 2–5 and 9–15 are denoted as $E_{\rm calc}$. Table 2 presents the experimental energies of states and the difference between the calculated and experimental energies for $^{220\text{-}224}$Th. For $^{226,\,228}$Th, $^{230,\,232}$Th, and $^{234,\,236}$Th, comparisons of the experimental and calculated energies are given in Table 3, Table 4, and Table 5, respectively. In almost all of these nuclei, the difference between the calculated and experimental energies does not exceed 1 keV, and for the $^{224,\,236}$Th nuclei, the calculated energy values differ from the experimental ones by a smaller amount than the experimental errors. Therefore, anomalies in the behavior of $J(\omega^2)$ for ^{236}Th in Fig. 2 should be attributed to the experimental errors. This anomaly disappears if the experimental value $E(4^+) = 160$keV is reduced by a value from 0.358 to 0.37 keV. Such high-quality descriptions of energies of states in the model of variable moment of inertia in heavy nuclei are obtained given that excitation energies can reach up to 5 MeV and the spin of states up to 30^+.

Most heavy nuclei have a stable deformation, and the deviation to the smaller side of the energies in the band from the dependence $I(I+1)$ has several causes, as partly

Table 2. Comparison of experimental [17] and theoretical energy values in keV for ^{220,222,224}Th nuclei.

I^π	^{220}Th		^{222}Th		^{224}Th	
	Exp.	$E_{\rm cal}-E_{\rm exp}$	Exp.	$E_{\rm cal}-E_{\rm exp}$	Exp.	$E_{\rm cal}-E_{\rm exp}$
2^+	386.5(1)	−0.001	182.9(2)	−0.06	98.1(3)	−0.12
4^+	759.80(15)	0.002	439.2(3)	0.22	284.1(5)	0.58
6^+	1166.03(17)	−0.002	749.3(4)	−0.29	534.7(5)	−0.30
8^+	1598.16(20)	−0.0005	1092.8(5)	0.09	833.9(6)	−0.46
10^+	2012.73(23)	38	1460.8(5)	−0.01	1173.8(6)	−0.01
12^+	2441.9(3)	78	1850.6(5)	−3.8	1549.8(6)	0.43
14^+	2885.0(3)	118	2259.7(6)	−12	1958.9(7)	0.21
16^+	3376.4(6)	121	2688.0(6)	−28	2398.0(7)	−0.27
18^+	3867.1(6)	136	3133.9(6)	−51	2864	0.01
20^+	4319.6(7)	198	3596.8(7)	−82		
22^+	4716.1(12)	324	4078.6(7)	−124		
24^+			4579.2(7)	−177		
26^+			5099.2(9)	−244		

Table 3. Comparison of experimental [17] and theoretical energy values in keV for ^{226,228}Th nuclei.

I^π	^{226}Th		^{228}Th	
	Exp.	$E_{cal}-E_{exp}$	Exp.	$E_{cal}-E_{exp}$
2^+	72.20(4)	−0.27	57.773(3)	0.17
4^+	226.43(5)	0.36	186.838(3)	0.08
6^+	447.3(2)	0.69	378.195(12)	−0.46
8^+	721.9(2)	0.38	622.5(3)	−0.85
10^+	1040.3(3)	−0.10	911.8(3)	−0.78
12^+	1395.2(4)	−0.24	1239.3(4)	−0.21
14^+	1781.5(5)	0.02	1599.4(5)	0.55
16^+	2195.8(6)	0.22	1987.9(6)	0.64
18^+	2635.1(7)	0.32	2400.5(8)	0.23
20^+	3097.1(8)	0.15	2834.4	−1.2
22^+			3283.4	−0.15

Table 4. Comparison of experimental [17] and theoretical energy values in keV for ^{230,232}Th nuclei.

I^π	^{230}Th		^{232}Th	
	Exp.	$E_{cal}-E_{exp}$	Exp.	$E_{cal}-E_{exp}$
2^+	53.230(11)	0.04	49.369(9)	0.02
4^+	174.119(17)	0.019	162.12(2)	0.08
6^+	356.54(12)	0.01	333.26(8)	0.29
8^+	593.89(17)	−0.27	556.9(1)	0.23
10^+	879.36(24)	−0.39	826.8(1)	−0.22
12^+	1206.7(5)	0.06	1137.1(5)	−0.95
14^+	1571.9(6)	−0.05	1482.2(6)	−1.1
16^+	1969.6(7)	0.13	1858.5(7)	−1.2
18^+	2396.4(9)	0.09	2262.4(9)	−0.56
20^+	2848.7(10)	0.09	2691(1)	0.95
22^+	3324.1(11)	−0.32	3144(1)	1.5
24^+	3819.1(15)	−0.05	3620.0(15)	0.89
26^+			4117(2)	−0.50
28^+			4633(2)	−1.8
30^+			5164(3)	−0.15

discussed earlier. This corresponds to the growth of the moment of inertia from the rotation frequency. The monotony of such a dependence at sufficiently large spins of states can be violated, leading, for example, to backbending, and this invariably occurs in medium nuclei. Additionally, an anomaly in the behavior of the moment of inertia can manifest itself through upbending, when the intersection of bands is not fully completed, and, finally, downbending. This effect can manifest itself at spins of at least 26^+ and in cases when, for example, a state with the same spin but in the S band becomes significantly higher

Table 5. Comparison of experimental [17] and theoretical energy values in keV for ^{234,236}Th nuclei.

I^π	^{234}Th		^{236}Th	
	Exp.	$E_{cal}-E_{exp}$	Exp.	$E_{cal}-E_{exp}$
2^+	49.55(6)	0.14	48.4(3)	0.09
4^+	163.05(12)	0.14	160.0(6)	−0.36
6^+	336.45(24)	−.24	329.4(7)	0.14
8^+	564.7(3)	−0.80	553.4(7)	−0.06
10^+	842.5(4)	−1.03	826.1(9)	−0.04
12^+	1164.9(6)	−0.81		
14^+	1526.6(7)	0.11		
16^+	1923.4(8)	0.80		
18^+	2351.0(9)	0.72		
20^+	2805.1(11)	−0.13		
22^+	3281.4(12)	−1.04		
24^+	3775.1(13)	−0.15		

and the observed state remains primarily collective. Moreover, the energies of such high-spin collective states may become somewhat higher than those that would be obtained based on the trends corresponding to lower spins. This behavior of the energies of collective states at high spins may have two causes. One is associated with the reduction of the configuration space of two-quasiparticle states that form the D phonon, in the presence of multibosons, which occurs to a greater extent at high spins. To quantitatively evaluate this phenomenon at the energy of collective states, we must obtain self-consistent solutions for each of the collective states separately, as performed for medium nuclei [9]. However, for heavy nuclei, such a procedure is difficult to implement owing to the high sensitivity of the calculated energies to the IBM Hamiltonian parameters. Another reason for additional growth of energies of collective states at high spins, which is what downbending provides, may be the specificity of the description of collective states in the general case of the $SU(6)$ symmetry, which consists in the finiteness of the maximum number of quadrupole bosons Ω.

In the variable moment of inertia model, the growth of the slope $J(\omega^2)$ is effectively reproduced. One of the reasons for this growth is the gradual increase of the noncollective component in the states of the yrast band. This explains why in deformed nuclei the quality of the description of energies in the Harris model is better than in the IBM phenomenology. The scenario regarding IBM changes if we move from its phenomenology to the microscopic version, when the IBM parameters are calculated and high-spin excitation modes are explicitly considered. This also enables us to determine the limits of applicability of the Harris scheme in the region of spins

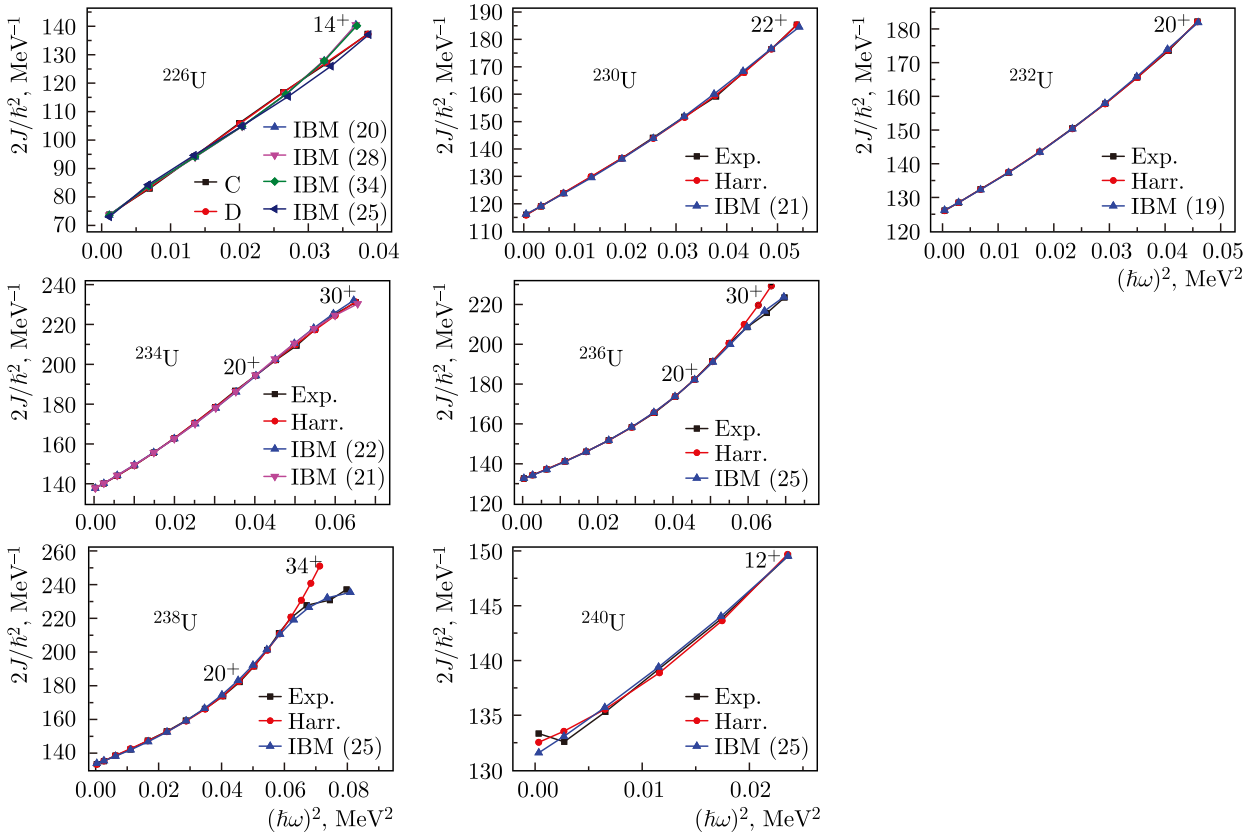

Fig. 5. (color online) Effective moments of inertia from experimental and theoretical energy values of yrast bands in U isotopes.

where the bands cross. For example, a microscopic calculation of the structure of the states of the yrast band in ^{222}Th [4] showed that the Harris scheme successfully reproduces collective states in which the collective component is noticeably larger than any of the others, and it can be somewhat less than 50%.

IV. ANALYSIS OF MOMENTS OF INERTIA FOR EVEN ISOTOPES OF U

The parameters determining the moment of inertia for U isotopes are given in Table 1. The corresponding moments of inertia are given in Fig. 5. In addition to the experimental and calculated values of the moments of inertia according to the Harris scheme, the results of calculations in accordance with the IBM phenomenology are given, excluding high-spin modes.

The parameters of the boson Hamiltonian (8) for the U isotopes are given in Table 6, and the corresponding moments of inertia with others are also given in Fig. 5. The parameters of the boson Hamiltonian given in Table 6 have an accuracy of 1 eV. To justify the need for such high accuracy, we calculated the partial derivatives $\partial E_I/\partial\varepsilon_d,\ldots,\partial E_I/\partial C_4$ in the vicinity of the parameter values determined for ^{236}U. They are given in Table 7. Based on these values, the maximum deviations of the parameters were obtained when the deviations of the calculated energies do not exceed 0.1 keV. These values are given in Table 8. The change in the Hamiltonian parameter (8) k_1 reacts most strongly to the energies of the states under consideration. As shown in Table 8, at high spins, its values should be given with greater accuracy than 1 eV, but because the experimental uncertainty of energies exceeds 1 keV at high spins, this can be avoided for now.

The IBM Hamiltonian parameters, including the Ω number for $^{226\text{-}238}$U were determined from states up to the limiting observed spins and are given in Table 6. Let us discuss the quality of the description of the energies of states consistently in all uranium isotopes under consideration.

For ^{226}U, the experimental data exhibit a practically linear dependence of $J(\omega^2)$, and this is naturally reproduced in the Harris scheme. This could not be obtained in the description in the IBM. The calculations were performed in a wide range of Ω from 14 to 34. In this case, if the quality of reproduction of energies for states with $I \le 12^+$ is satisfactory, as evident from Table 9, where the values of energies with $\Omega = 20$ are given, the energy of the state with 14^+ becomes underestimated by 7 keV. This leads to the increase in the calculated value of J. If we degrade the quality of the energy description, the linear dependence $J(\omega^2)$ is approximately reproduced, which is re-

Table 6. IBM Hamiltonian parameters for ^{226}Th even U nuclei.

Nucleus	ε_d	k_1	k_2	C_0	C_2	C_4	Ω
^{226}Th	0.367969	-0.030993	0.003373	-0.080729	-0.022919	-0.035625	28
^{226}U	−0.080461	−0.030253	0.009227	0.005134	0.060668	0.001103	20
^{226}U	0.036599	−0.038003	0.004841	−0.010224	0.033211	−0.034492	28
^{226}U	0.040505	−0.036817	0.004122	0.136447	0.035798	−0.031713	34
^{226}U	−0.059896	−0.037406	0.004168	0.001010	0.011875	−0.020448	25
^{230}U	−0.614828	−0.058595	0.032967	0.899961	0.061097	0.045202	21
^{232}U	−0.725962	−0.058227	0.032505	0.739341	0.034253	0.054798	19
^{234}U	−0.594347	−0.049232	0.032013	0.674469	0.076536	0.039112	22
^{234}U	−0.580119	−0.049519	0.034100	0.637994	0.071404	0.038430	21
^{236}U	−0.626829	−0.059598	0.051147	0.713640	0.042979	0.019237	25
^{238}U	−0.634858	−0.060349	0.053701	0.687343	0.039218	0.016058	25
^{240}U	−0.634453	−0.059500	0.050521	0.717118	0.029825	0.022396	25

Table 7. Partial derivatives of IBM energies with respect to boson parameters in the special case of parameters adopted for ^{236}U; $E_{I\geq 2}$ represents the excitation energy, and E_0 is the total boson energy, measured from the energy of the d-boson vacuum.

I^π	0^+	2^+	4^+	6^+	8^+	10^+	12^+	14^+	16^+	18^+	20^+	22^+	24^+	26^+	28^+	30^+
$\partial E_I/\partial\varepsilon_d$	11	0.071	0.23	0.48	0.8	1.2	1.7	2.2	2.7	3.3	4.0	4.7	5.4	6.2	6.9	7.7
$\partial E_I/\partial k_1$	316	−2.5	−8.1	−16.7	−28	−41.7	−57.4	−74.8	−93.7	−113	−134	−155	−175	−196	−216	−234
$\partial E_I/\partial k_2$	−138	0.475	−1.54	−3.09	−5.0	−7.1	−9.3	−11.4	−13.4	−15	−16	−16.6	−16.3	−15.2	−13	−9.5
$\partial E_I/\partial C_0$	12	−0.067	−0.23	−0.47	−0.8	−1.21	−1.7	−2.2	−2.9	−3.6	−4.2	−5.1	−5.8	−6.6	−7.4	−8.2
$\partial E_I/\partial C_2$	−17	0.071	0.23	0.48	0.8	1.19	1.7	2.2	2.7	3.3	3.9	4.6	5.3	6.0	6.7	7.3
$\partial E_I/\partial C_4$	23	0.65	2.16	4.55	7.8	11.9	17.0	22.9	29.6	37.4	46.0	55.6	66.2	77.7	90.2	104

Table 8. Required accuracy of the parameters in eV for the accuracy of calculating the energy of the yrast band states to be not less than 0.1 keV in the particular case of the parameters adopted for ^{236}U; for $I\neq 0$, the energies are considered relative to the ground state.

I^π	0^+	2^+	4^+	6^+	8^+	10^+	12^+	14^+	16^+	18^+	20^+	22^+	24^+	26^+	28^+	30^+
$\triangle\varepsilon_d$	9	1400	430	210	125	83	59	45	37	30	25	21	18	10	14	13
$\triangle k_1$	0.32	40	12	6	3.6	2.4	1.7	1.3	1.1	0.88	0.75	0.65	0.57	0.51	0.46	0.43
$\triangle k_2$	0.72	210	65	32	20	14	11	8.8	7.5	6.7	6.2	6.0	6.1	6.6	7.7	10
$\triangle C_0$	8	1492	435	213	125	83	59	45	34	28	24	20	17	15	14	12
$\triangle C_2$	6	1408	435	208	125	84	59	45	37	30	26	22	19	17	15	14
$\triangle C_4$	4	154	46	22	13	8.4	5.9	4.4	3.4	2.7	2.2	1.8	1.5	1.3	1.5	1.3

flected in Fig. 5. The question of the possibility of quantitative reproduction of the energies of the ^{226}U nucleus in IBM remains open, despite the question concerning the description of states up to relatively low spins. Note that the experimental errors for this isotope are the highest of all those considered.

For the next nucleus, ^{230}U, the description of energies in the Harris scheme is precise, and the difference between the calculated and experimental values of energies, as shown in Table 10, does not exceed 0.4 keV. Within the IBM framework, this is 1.4 keV, which also indicates a high quality of the description, despite the states being observed up to 22^+.

For ^{232}U, states are observed up to 20^+, and the description of their energies in the two calculations is quite satisfactory. Thus, in the Harris scheme, the discrepancy is no more than 0.21 keV, and for the IBM, it is no more than 1.2 keV, as noted in Table 11. The quality of the energy description is particularly clearly manifested through the moments of inertia for ^{230}U and ^{232}U in Fig. 5.

For ^{234}U, states are observed already up to 30^+. In the Harris scheme, the discrepancy is no more than 0.86 keV. Within the IBM framework, as shown in Fig. 5, calculations were made with two values of Ω: 21 and 22. The

Table 9. Comparison of experimental [17] and theoretical energy values in keV for ^{226}U nuclei; for the IBM, $\Omega = 20$.

I^π	^{226}U				
	Exp.	$E_{\rm cal}$	$E_{\rm cal} - E_{\rm exp}$	$E_{\rm IBM}$	$E_{\rm IBM} - E_{\rm exp}$
2^+	81.3(6)	81.464	0.16	81.510	0.21
4^+	250.0(9)	249.682	−0.32	248.46	−1.54
6^+	483.2(9)	482.79	−0.41	482.24	−0.92
8^+	766.4(10)	766.51	0.11	768.45	2.05
10^+	1091.6(10)	1091.98	0.38	1095.9	4.3
12^+	1453.8(10)	1453.42	−0.38	1455.7	1.9
14^+	1847.0(13)	1846.93	−0.07	1840.1	−6.9

Table 10. Comparison of experimental [17] and theoretical energy values in keV for ^{230}U nuclei; for the IBM, $\Omega = 21$.

I^π	^{230}U				
	Exp.	$E_{\rm cal}$	$E_{\rm cal} - E_{\rm exp}$	$E_{\rm IBM}$	$E_{\rm IBM} - E_{\rm exp}$
2^+	51.737(23)	51.797	0.060	51.623	−0.114
4^+	169.35(4)	169.356	0.006	169.17	−0.18
6^+	346.96(20)	346.85	−0.11	347.04	0.08
8^+	578.1(3)	577.76	−0.34	578.59	0.49
10^+	856.3(3)	855.91	−0.39	857.24	0.94
12^+	1175.6(4)	1175.68	0.08	1177.0	1.40
14^+	1531.5(4)	1532.07	0.57	1532.7	1.20
16^+	1921.0(5)	1920.65	−0.35	1920.1	−0.90
18^+	2337.6(6)	2337.56	−0.04	2335.9	−1.7
20^+	2779.6(11)	2779.47	−0.13	2777.6	−2.0
22^+	3243.6(15)	3243.54	−0.06	3243.7	0.1

results of the calculations of the moments of inertia closely cover the moments of inertia from the experimental energies on both sides. Considering the influence of high-spin modes on the energies of states, we give preference to $\Omega = 21$, for which the calculated values are presented in Table 12. The table clearly shows that the corresponding differences are no more than 3.2 keV.

In the ^{236}U nucleus, the observed states also extend to $I = 30^+$. The observed moments of inertia at $I = 28^+$ and $I = 30^+$ result in a decrease in the slope of $J(\omega^2)$. More precisely, starting from spin 26^+, a slower growth of the moment of inertia—downbending—is manifested. This is why the parameters in the Harris scheme are determined by the states up to spin $I = 24^+$, and for these states, the difference between the experimental and calculated energies does not exceed 0.74 keV, as follows from Table 13. The moments of inertia at high spins, as shown in Fig. 5, for this nucleus significantly exceed the experimental values. The calculation in the IBM reproduces this experimental trend, and this is achieved at $\Omega = 25$. This can be

Table 11. Comparison of experimental [17] and theoretical energy values in keV for ^{232}U nuclei; for the IBM, $\Omega = 19$.

I^π	^{232}U				
	Exp.	$E_{\rm cal}$	$E_{\rm cal} - E_{\rm exp}$	$E_{\rm IBM}$	$E_{\rm IBM} - E_{\rm exp}$
2^+	47.573(8)	47.590	0.017	47.533	−0.04
4^+	156.566(10)	156.545	−0.021	156.49	−0.076
6^+	322.69(7)	322.76	0.065	322.80	0.11
8^+	541.1(1)	540.97	−0.13	541.23	0.13
10^+	805.88(16)	805.68	−0.20	806.16	0.28
12^+	1111.6(2)	1111.59	−0.01	1112.1	0.50
14^+	1453.8(3)	1453.91	0.10	1454.1	0.30
16^+	1828.2(4)	1828.39	0.19	1828.0	−0.20
18^+	2231.6(6)	2231.39	−0.21	2230.4	−1.2
20^+	2659.8(9)	2659.78	−0.02	2659.3	−0.5

Table 12. Comparison of experimental [17] and theoretical energy values in keV for ^{234}U nuclei; for the IBM, $\Omega = 21$.

I^π	^{234}U				
	Exp.	$E_{\rm cal}$	$E_{\rm cal} - E_{\rm exp}$	$E_{\rm IBM}$	$E_{\rm IBM} - E_{\rm exp}$
2^+	43.4981(10)	43.501	0.003	43.517	−0.195
4^+	143.352(4)	143.362	0.010	143.34	1.92
6^+	296.072(4)	296.12	0.046	295.89	0.97
8^+	497.04(3)	497.06	0.02	496.63	0.17
10^+	741.2(5)	741.13	−0.07	740.75	0.54
12^+	1023.8(7)	1023.56	−0.24	1023.6	0.60
14^+	1340.5(12)	1340.22	−0.28	1340.9	1.50
16^+	1687.8(16)	1687.70	−0.1	1689.1	1.90
18^+	2062.8(17)	2063.20	0.4	2064.9	2.20
20^+	2464.0(18)	2464.49	0.49	2465.9	2.30
22^+	2889.5(18)	2889.78	0.28	2890.3	2.0
24^+	3338.5(21)	3337.64	−0.86	3336.9	1.9
26^+	3807.5(23)	3806.98	−0.52	3805.0	3.2
28^+	4296.5(25)	4296.95	0.45	4294.8	3.2
30^+	4807	4806.98	−0.02	4807.1	3.2

associated with a decrease in the collective configuration space at the corresponding spins, as well as the presence of s bosons or square roots, owing to which the closure of the $SU(6)$algebra of boson operators is achieved in comparison with other collective models. This is the case when the variable moment of inertia model with the used parameterization cannot describe this phenomenon, and the IBM phenomenology describes the corresponding increase in the energies of collective states. Such a phenomenon occurs, as can be determined by $^{236,\,238}$U nuclei, starting with spin 28^+. For all states of this nucleus, the difference between the calculated IBM and experimental

energy values does not exceed 2 keV.

The effect observed in the ^{236}U nucleus of weakening the growth of J from ω^2 at $I = 28^+$, 30^+ is even more pronounced in the ^{238}U nucleus as the spins observed for it extend to $I = 34^+$. The parameters in the Harris scheme are determined by the states with $I \leq 28^+$. For these states, as shown in Table 14, the difference between the experimental and calculated energies does not exceed 0.76 keV. For large spins, this difference increases rapidly, and the calculated energy values are noticeably lower than the experimental ones. As shown in Fig. 5, for this nucleus, the calculation in the IBM reproduces the experimental scenario, and this is achieved at $\Omega = 25$. If we use large values of Ω, for example, 30, J will be significantly larger, approaching values given by the Harris scheme. The difference between the experimental and calculated energies within the IBM framework for all spins does not exceed 4.6 keV.

Note that the description of the energies of states in a number of uranium nuclei is highly effective such that the discrepancies with experimental values occasionally provide smaller values than the experimental uncertainties, particularly for calculations in the Harris scheme.

As a rule, the quality of description in the Harris model is higher than that in the IBM. This is evident from ^{226,230,232,234}U (no experimental data exist for ^{228}U). This can be explained by the method of determining the parameters. For the Harris scheme, they are determined using the least squares method, which makes them clearly optimal, whereas for the IBM, other methods for determining the parameters must be used, which are not as effective. For ^{236}U, as shown inFig. 5, both models reproduce the energies equally qualitatively.

For ^{240}U, states are known only up to spin 12^+. In Fig. 5, for ^{240}U, a strong anomaly of the moment of inertia for the first excitation is visible. It cannot be reproduced by any of the models, and its presence is associated with a large experimental error in the energy of the first excitation (see Table 15). When describing energies within the IBM framework, if the parameters are determined without the 2_1^+ state, the corresponding energy becomes equal to 45.6 keV, that is, 0.6 keV higher than that suggested by the experiment. In this case, the experimental error for this state is equal to 1 keV, *i.e.*, such a correction is within the experimental corridor of admissible values, and the anomaly in the effective moment of inertia is the result of a large experimental uncertainty. If the moments of inertia are determined with the corrected energy of the 2^+ state, the value of σ decreases significantly and becomes equal to 0.08.

V. CONCLUSIONS

A comparison of the effective moments of inertia for heavy even nuclei, namely, thorium and uranium isotopes, with the variable moment of inertia model and IBM, each in its phenomenological aspect and micro-

Table 13. Comparison of experimental [17] and theoretical energy values in keV for ^{236}U nuclei; for the IBM, $\Omega = 25$.

I^π	^{236}U				
	Exp.	E_{cal}	$E_{cal} - E_{exp}$	E_{IBM}	$E_{IBM} - E_{exp}$
2^+	45.2431(20)	44.915	−0.33	45.204	−0.0391
4^+	149.480(5)	148.921	−0.56	149.43	−0.05
6^+	309.788(6)	309.85	0.062	309.87	0.082
8^+	522.26(4)	523.77	1.5	522.58	0.32
10^+	782.4(5)	785.39	2.99	782.93	0.53
12^+	1085.4(7)	1088.97	3.6	1086.0	0.6
14^+	1426.4(9)	1429.25	2.8	1426.8	0.4
16^+	1801.0(10)	1801.74	0.74	1800.8	−0.2
18^+	2204.0(12)	2202.78	−1.2	2203.7	−0.3
20^+	2631.8(13)	2629.43	−2.4	2631.7	−0.1
22^+	3081.0(14)	3079.34	−1.7	3081.9	0.9
24^+	3550.0(17)	3550.57	0.57	3552.0	2.0
26^+	4039.0(20)	4041.55	2.6	4040.9	1.9
28^+	4549.0(22)	4550.99	1.99	4548.4	−0.6
30^+	5077(4)	5077.80	0.8	5075.8	−1.2

Table 14. Comparison of experimental [17] and theoretical energy values in keV for ^{238}U nuclei; for the IBM, $\Omega = 25$.

I^π	^{238}U				
	Exp.	E_{cal}	$E_{cal} - E_{exp}$	E_{IBM}	$E_{IBM} - E_{exp}$
2^+	44.916(13)	45.004	0.0883	44.785	−0.131
4^+	148.38(3)	148.394	0.014	148.10	−0.28
6^+	307.18(8)	307.12	−0.057	307.26	0.08
8^+	518.1(3)	517.45	−0.65	518.49	0.31
10^+	775.9(4)	775.32	−0.58	777.25	1.35
12^+	1076.7(5)	1076.38	−0.32	1078.7	2.0
14^+	1415.5(6)	1415.94	0.44	1417.9	2.4
16^+	1788.4(6)	1789.15	0.75	1790.1	1.7
18^+	2191.1(7)	2191.41	0.31	2191.0	−0.1
20^+	2619.1(8)	2618.62	−0.48	2616.7	−2.4
22^+	3068.1(9)	3067.34	−0.76	3064.1	−4.1
24^+	3535.3(12)	3534.76	−0.54	3530.7	−4.6
26^+	4018.1(16)	4018.57	0.47	4015.1	−3.0
28^+	4517	4516.92	−0.084	4517.1	0.1
30^+	5035.1(21)	5028.27	−6.83	5038.0	2.9
32^+	5581(3)	5551.37	−29.6	5580.7	−0.3
34^+	6146(4)	6085.16	−60.8	6149.9	3.9

Table 15. Comparison of experimental [17] and theoretical energy values in keV for ^{240}U nuclei; for the IBM, $\Omega = 25$.

I^{π}	^{240}U				
	Exp.	$E_{\rm cal}$	$E_{\rm cal} - E_{\rm exp}$	$E_{\rm IBM}$	$E_{\rm IBM} - E_{\rm exp}$
2^+	45(1)	45.274	0.27	45.599	0.6
4^+	150.60(10)	150.112	−0.49	150.80	0.2
6^+	313.19(14)	312.41	−0.78	312.91	−0.28
8^+	528.69(18)	528.43	−0.26	528.12	−0.57
10^+	792.9(3)	793.00	0.1	791.95	−0.95
12^+	1100.5(4)	1100.32	−0.18	1099.6	−0.9

scopic version, enabled us to draw the following conclusions.

1. The Harris model effectively reproduces the experimental situation if the collective component in the wave function remains at least 50%. The standard boson model cannot do this; hence, it must be extended by explicitly considering high-spin excitation modes up to $J \leq 14^+$. However, the Harris scheme does not reproduce the decrease in the slope of J from ω^2.

2. If the energies of collective states increase significantly at spins greater than 28^+, this may be because of a reduction in the collective configuration space. This scenario is reproduced in the IBM phenomenology but cannot be reproduced in either the Harris model or classical geometric collective models.

In this study, the Harris scheme is not considered through the use of the cracking model but only as one of the convenient and visual representations of the excitation energies in the bands. In a number of cases for the lowest states, when large experimental uncertainties exist, the scheme can provide clarifying estimates. For large values of spins, when the experimental values of the moments of inertia are noticeably greater than the Harris estimates, we can make judgments about the extent of the influence of noncollective modes with high spins on these states.

References

[1] S.M. Harris, Phys. Rev. B **138**(3), 509 (1965)
[2] A.D. Efimov and I.N. Izosimov, Phys. At. Nucl. **84**(5), 660 (2021)
[3] A. Arima and F. Iachello, Phys. Rev. Lett. **35**, 1069 (1975)
[4] A.D. Efimov and I.N. Izosimov, Int. J. Mod. Phys. E **34**, 2541004 (2025) ; JINR Preprint E4-2024-27. Dubna, 2024
[5] N. Yoshida, H. Sagawa, T. Otsuka *et al.*, Phys. Lett. B **256**(2), 129 (1991)
[6] Y.-X. Liu, J.-G. Song, H.-Z. Sun *et al.*, Phys. Rev. C **56**(3), 1370 (1997)
[7] Y. Liu, J. Song, S H. Zhou *et al.*, J. Phys. G: Nucl. Part. Phys. **24**, 117 (1998)
[8] A. Dadwal and X.-T. He, arXiv: 2403.05823v1
[9] A.D. Efimov, Phys. At. Nucl. **83**(5), 651 (2020)
[10] A. D. Efimov and V. M. Mikhajlov, Bull. Russ. Acad. Sci.: Phys. **76**(8), 857 (2012)
[11] A. D. Efimov and V. M. Mikhajlov, Bull. Russ. Acad. Sci.: Phys. **75**(7), 890 (2011)
[12] A.D. Efimov, I.V. Koval, I.N. Izosimov, P. N. Usmanov, JINR Preprint E4-2024-61. Dubna, 2024
[13] Y. Zhao, X. Z. Kang, S. F. Shen *et al.*, Chin. Phys. Lett. **29**(5), 052101 (2012)
[14] A.V. Afanasjev, Phys. Scr. **89**, 054001 (2014)
[15] F.A. Jaafer and F.H. Al-Khudair, Phys. Rev. C **106**, 064309 (2022)
[16] A. D. Efimov and I. N. Izosimov, Phys. At. Nucl. **86**(4), 333 (2023)
[17] National Nuclear Data Center, Brookhaven National Laboratory. http://www.nndc.bnl.gov.